**Supplemental Information**

Brown Adipose Tissue Activation Is Linked

to Distinct Systemic Effects

on Lipid Metabolism in Humans

Maria Chondronikola, Elena Volpi, Elisabet Børsheim, Craig Porter, Manish K. Saraf, Palam Annamalai, Christina Yfanti, Tony Chao, Daniel Wong, Kosaku Shinoda, Sebastien M. Labbè, Nicholas M. Hurren, Fernardo Cesani, Shingo Kajimura, and Labros S. Sidossis
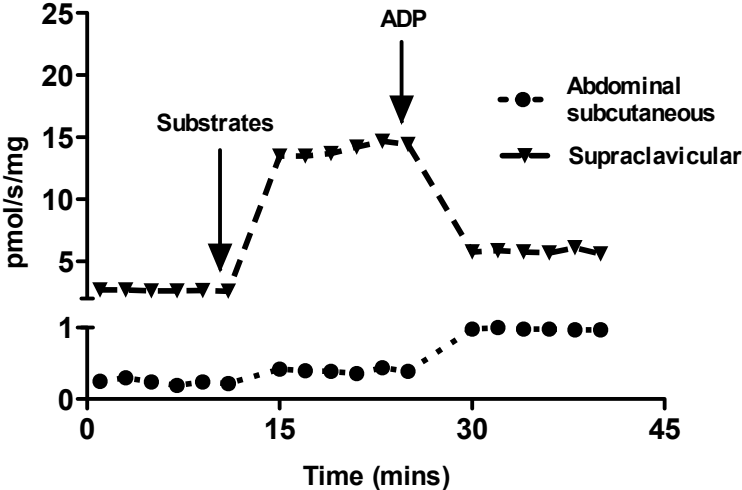
SUPPLEMENTAL DATA ITEMS

Figure S1. Study Design (related to Figure 1)
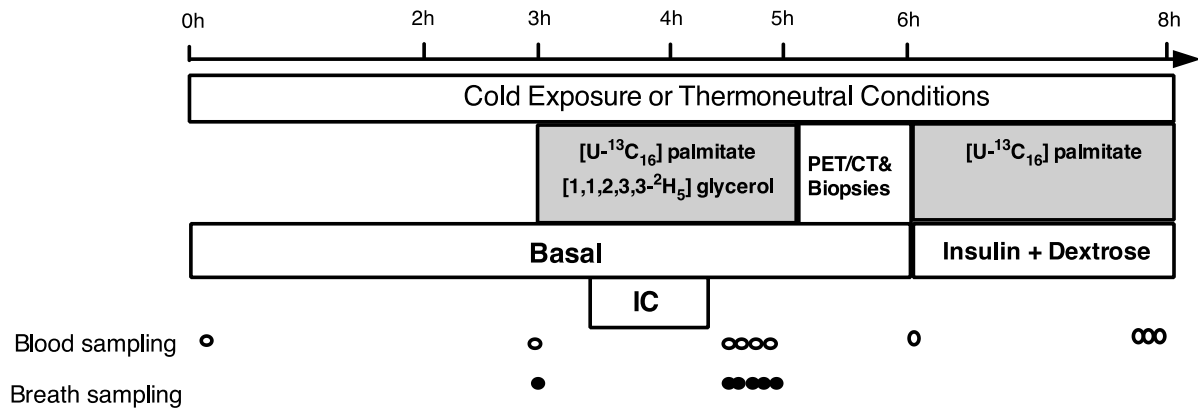
Figure S1

PET/CT: positron emission tomography/ computed tomography; IC: indirect calorimetry.

Figure S2. Oxygen consumption trace in supraclavicular brown and abdominal subcutaneous adipose tissue biopsies (related to Figure 1)

Table S1. Correlation matrix of muscle metabolic activity with cold-induced change in whole-body lipid kinetics (related to Figure 1)

	Muscle mean SUV
Cold-induced change in FFA oxidation (µmol/kg/min)	r = -0.2 p = 0.6
Cold-induced change in lipolysis (µmol/kg/min) [a]	r = 0.03 p = 0.9
Cold-induced change in TG-FFA cycling (µmol/kg/min)	r = 0.2 p = 0.6
Cold-induced change in adipose tissue insulin sensitivity (%) [b]	r = -0.3 p = 0.3

[a] Expressed as glycerol rate of appearance. [b] Adipose tissue insulin sensitivity was calculated as the % suppression on palmitate rate of appearance with insulin. FFA: free fatty acid, SUV: standardized uptake value, TG: triglycerides.

Table S2. Plasma lipid and lipoprotein concentrations during cold exposure (CE) and thermoneutral (TN) conditions (related to Figure 1).

	TN	CE
FFA (μmol/ml)	0.43 ± 0.22	0.63 ± 0.28**
Glycerol (μmol/ml)	0.07 ± 0.04	0.09 ± 0.04*
TG (mg/dl)	135 ± 76	139 ± 97
TCHOL (mg/dl)	158 ± 26	169 ± 44
LDL-C (mg/dl)	97 ± 20	105 ± 33
HDL-C (mg/dl)	35 ± 11	36 ± 10

Data are means ± SD. FFA: free fatty acid; TG: triglycerides; TCHOL: total cholesterol; LDL-C: low-density lipoprotein-cholesterol; HDL-C: high-density lipoprotein-cholesterol; * $p=0.01$, ** $p=0.005$ between CE and TN using paired t-test.

Table S3. Plasma lipid and lipoprotein concentrations 14 h after each metabolic study (related to Figure 1)

	TN	CE
TG (mg/dl)	160 ± 82	127 ± 63*
TCHOL (mg/dl)	180 ± 28	176 ± 31
VLDL-C (mg/dl)	32 ± 16	25 ± 13*
LDL-C (mg/dl)	108 ± 28	108 ± 36
HDL-C (mg/dl)	40 ± 13	41 ± 10
non HDL-C (mg/dl)	140 ± 28	140 ± 28
TG: HDL-C ratio	4.8 ± 3.7	3.6 ±2.1
TCHOL:HDL-C ratio	4.9 ± 1.6	4.7 ± 1.3
LDL$_{NMR}$: HDL$_{NMR}$ ratio	42.5 ± 15.2	40.5 ± 10.2
sLDL$_{NMR}$: lHDL$_{NMR}$ ratio	258 ± 246	234 ± 141

Data are means ± SD. TN: thermoneutral conditions; CE: cold exposure; TG: triacylglycerol; TCHOL: total cholesterol; VLDL-C: very low-density lipoprotein cholesterol; LDL-C: low density lipoprotein-cholesterol; HDL-C: high density lipoprotein-cholesterol; LDL$_{NMR}$: low density lipoprotein particle concentration; HDL$_{NMR}$: high density lipoprotein particle concentration; sLDL$_{NMR}$: small low density lipoprotein particle concentration; lHDL$_{NMR}$: large high density lipoprotein particle concentration. * $p=0.01$ between CE and TN using paired t-test.

SUPPLEMENTAL EXPERIMENTAL PROCEDURES

Biopsies

Adipose tissue samples (100-150 mg) from the supraclavicular and abdominal areas were obtained using a suction adapted Bergström needle technique, as previously described (Chondronikola et al., 2015). The exact location of the supraclavicular biopsy was determined by the ^{18}F-FDG-PET/CT images showing activated BAT (during the CE trial). Depending on the availability, one piece of the biopsy was snap-frozen for real-time quantitative PCR analysis, while the other was prepared to determine mitochondrial respiration.

Individualized Cold Exposure (CE) Protocol

Subjects were studied in a room with an ambient temperature of ~19°C and wearing garments cooled by liquid circulation (Cool Flow® vest and blanket, Stow, OH). The temperature of the vest was initially set at 20°C, then decreased in 1°C intervals through an air-conditioned temperature control bath (Chiller Reservoir System, Polar Products Inc., Stow, OH) until subjects reported shivering. At this point, the vest and room temperature was increased by ~1°C and was maintained constant or titrated as needed to prevent shivering.

Positron Emission Tomography/Computed Tomography (PET/CT)

After 5 h of exposure to cold (CE) or thermoneutral (TN) conditions, subjects were injected with a bolus of 185 MBq of 2-Deoxy-2-[18F]fluoroglucose (^{18}F-FDG). One hour later, we performed a PET/CT (GE Discovery ST 4 Slice, General, Electric, Milwaukee, WI) scan to assess brown adipose tissue (BAT) volume and total BAT glucose disposal [*BAT volume (ml) * mean standardized disposal value, g/ml (SUV)*]. An independent investigator blinded to the status of the participants assessed the PET/CT scans for BAT using the following criteria: (a) ^{18}F-FDG disposal evident in the cervical/supraclavicular, mediastinal, paravertebral, and/or perirenal areas; (b) ^{18}F-FDG disposal with mean SUV≥1.5 (an indicator of ^{18}F-FDG disposal intensity); and (c) the tissue corresponded to the density of adipose tissue on CT (−190 to −30 Hounsfield Units) (Borel et al., 2012; Ferland et al., 1989; Pare et al., 2001). The mean SUVs for each identified depot were determined using commercial fusion software (MIM software; MIMvista Corp., Cleveland, OH). The volume of ^{18}F-FDG BAT was quantified by auto-contouring each identified individual BAT depot.

Body Composition

We used Dual-emission X-Ray Absorptiometry (GE Lunar iDXA, GE Healthcare, Little Chalfont, Buckinghamshire, UK) to evaluate the lean body mass and fat mass of participants (Hologic model QDR-4500W, Hologic Inc., Bedford, MA).

Indirect calorimetry

We determined oxygen consumption and carbon dioxide production rates using indirect calorimetry (Vmax Encore[TM], CareFusion Corp., San Diego, CA). Equipment failure occurred in two participants.

Mitochondrial Respiration

A portion of each adipose tissue biopsy was immediately transferred to an ice-cold preservation buffer after collection (10 mM EGTA containing 6.6 mM $MgCl_2$, 50 mM MES, 0.5 mM Dithiothreitol, 20 mM Taurine, 20 mM Imidazole, 5.8 mM ATP, and 15 mM PCr) and stored on ice. Samples were immediately transferred to the laboratory where they were blotted on filter paper and weighed. Thereafter, approximately 25-50 mg of WAT or 5-10 mg of BAT were transferred to Oxygraph respirometer chambers (Oroboros Instruments, Innsbruck, Austria) and suspended in 2 ml of mitochondrial respiration buffer (0.5 mM EGTA buffer containing 20 mM HEPES, 3 mM $MgCl_2$, 10 mM potassium phosphate, 60 mM potassium lactobionate, 20 mM taurine, 110 mM sucrose, and 1 g/l bovine serum albumin). Adipose tissue was permeabilized by the addition of 2μM digitonin directly into the respirometer chamber, as described previously (Kraunsoe et al., 2010; Porter et al., 2015; Sidossis et al., 2015). Once the O_2 consumption signal had stabilized, a background leak respiratory rate was recorded (basal). Thereafter, substrates (1.5 mM octanoyl-carnitine, 5 mM pyruvate, 10 mM glutamate and 2 mM malate) were titrated into the chamber and State 2 (leak) respiration was recorded. Then, 5 mM ADP was titrated into the Oxygraph chamber to transition to State 3 (coupled) respiration. All measurements were made at 37°C, and O_2 concentration was maintained between 100-300 nmol/ml for all respirometry measurements.

RNA isolation, cDNA synthesis and quantitative real-time PCR

Approximately 50-100 mg of adipose tissue was used for extraction of RNA using a pure link RNA Isolation Mini Kit Total (Life Technologies, Carlsbad, CA) or RNeasy Lipid Tissue Mini Kit (Qiagen Inc., Valencia,

CA), including an on-column DNAse digestion step. cDNA was synthesized by High-Capacity RNA-to-cDNA™ Kit (Life Technologies, Carlsbad, CA) and pre-amplified by TaqMan® PreAmp Master Mix Kit (Life Technologies, Carlsbad, CA). Quantitative real-time-PCR analyses were performed on an ABI PRISM 7900HT using the TaqMan® Gene Expression Master Mix (Life Technologies, Carlsbad, CA) with pre-amplified cDNA and specific Taqman gene expression assays (Life Technologies, Carlsbad, CA). GAPDH was used as the housekeeping gene to normalize the expression of the target gene.

Transcriptional analysis

Approximately 100 mg of adipose tissue was used for extraction of RNA using a pure link RNA isolation mini kit (Life Technologies, Carlsbad, CA). RNA quality (RIN: RNA Integrity Number) was determined by Bioanalyzer (Agilent Technologies, Santa Clara, CA) and samples with a RIN of at least of 5 were subjected to RNA-seq. Libraries were constructed as previously described (Shinoda et al., 2015). High-throughput sequencing was performed using a HiSeq 2500 (Illumina) at the University of California San Francisco Center for Advanced Technology. Quality control checks on the raw sequence data was done by FastQC (The Babraham Bioinformatics) and adapter trimming was performed by Skewer (Jiang et al., 2014). Raw sequences were mapped using TopHat version 2.0.8 against the human (hg19) genome. The mapped sequences were converted to fragments per kilobase of exon per million fragments mapped (FPKM) by running Cuffdiff 2.1.1 to determine gene expression. The FPKM values were z-scored and visualized as a heat-map representation in the blue-white-red scheme by using Multi Experiment Viewer (Saeed et al., 2003). Gene set enrichment analysis was performed in ConsensusPathDB (Kamburov et al., 2009).

Blood Samples

We quantified individual and total plasma FFA concentrations via gas chromatography coupled to a flame ionization detector (GC-FID 6890; Hewlett-Packard / Agilent Technologies, Santa Clara, CA) after the addition of heptadecanoic acid to plasma as an internal standard. To quantify plasma enrichments of glycerol and palmitate, we used gas chromatography coupled to mass spectrometry (GC/MS 5975C, Hewlett-Packard / Agilent Technologies, Santa Clara, CA). Lipoprotein subclass particle concentrations and the average size of lipoprotein particles were determined by proton nuclear magnetic resonance spectroscopy (MRS) of whole plasma (LipoScience Inc., Raleigh,

NC) (Otvos et al., 2002). Total, HDL-, VLDL-, and LDL-cholesterol and triglyceride (TG) concentrations were quantified using a biochemical analyzer (Vitros 5600, Ortho Clinical Diagnostics, Inc., Rochester, NY). Plasma free triodothyronine concentrations were measured using chemiluminescence (Dxi 600, Beckman Coulter, Pasadena, CA). Serum leptin was measured using a multiplex assay (Milliplex, Billerica, MA).

Calculations

An isotopic steady state was achieved during the last 10 min of the basal and insulin clamp periods. The rates of appearance (R_a) of glycerol and palmitate were calculated using the following formula: tracer infusion rate / tracer-to-tracee ratio (Wolfe and Chinkes, 2005). Plasma FFA R_a FFA was calculated by dividing the R_a for palmitate by the fractional contribution of palmitate to the total FFA concentration. The whole-body lipolytic rate was estimated from R_a for glycerol and FFA.

Plasma palmitate oxidation rates were calculated as: $(ECO_2 * VCO_2)/(Eo * ar * 16)$, where ECO_2 = breath CO_2 carbon enrichment by isotope ratio mass spectrometry (Agilent Technologies, Santa Clara, CA), VCO_2 = the rate of elimination of CO_2, Eo = [U-$^{13}C_{16}$] palmitate enrichment in plasma, and ar = the acetate correction factor (Sidossis et al., 1996). Plasma FFA oxidation was determined by dividing the palmitate oxidation rate by the fractional contribution of palmitate to the total FFA concentration. Adipose tissue insulin sensitivity was calculated as the suppression of palmitate R_a with insulin (Fabbrini et al., 2012). TG-FFA cycling was calculated as the difference between 3 × the glycerol R_a and total fatty acid oxidation via indirect calorimetry (Wolfe and Chinkes, 2005).

SUPPLEMENTAL REFERENCES

Borel, A.L., Nazare, J.A., Smith, J., Almeras, N., Tremblay, A., Bergeron, J., Poirier, P., and Despres, J.P. (2012). Visceral and not subcutaneous abdominal adiposity reduction drives the benefits of a 1-year lifestyle modification program. Obesity (Silver Spring) *20*, 1223-1233.

Chondronikola, M., Annamalai, P., Chao, T., Porter, C., Saraf, M.K., Cesani, F., and Sidossis, L.S. (2015). A percutaneous needle biopsy technique for sampling the supraclavicular brown adipose tissue depot of humans. Int J Obes (Lond).

Fabbrini, E., Magkos, F., Conte, C., Mittendorfer, B., Patterson, B.W., Okunade, A.L., and Klein, S. (2012). Validation of a novel index to assess insulin resistance of adipose tissue lipolytic activity in obese subjects. J. Lipid Res. *53*, 321-324.

Ferland, M., Despres, J.P., Tremblay, A., Pinault, S., Nadeau, A., Moorjani, S., Lupien, P.J., Theriault, G., and Bouchard, C. (1989). Assessment of adipose tissue distribution by computed axial tomography in obese women: association with body density and anthropometric measurements. Br. J. Nutr. *61*, 139-148.

Jiang, H., Lei, R., Ding, S.W., and Zhu, S. (2014). Skewer: a fast and accurate adapter trimmer for next-generation sequencing paired-end reads. BMC bioinformatics *15*, 182.

Kamburov, A., Wierling, C., Lehrach, H., and Herwig, R. (2009). ConsensusPathDB--a database for integrating human functional interaction networks. Nucleic Acids Res *37*, D623-628.

Kraunsoe, R., Boushel, R., Hansen, C.N., Schjerling, P., Qvortrup, K., Stockel, M., Mikines, K.J., and Dela, F. (2010). Mitochondrial respiration in subcutaneous and visceral adipose tissue from patients with morbid obesity. The Journal of physiology *588*, 2023-2032.

Otvos, J.D., Jeyarajah, E.J., and Cromwell, W.C. (2002). Measurement issues related to lipoprotein heterogeneity. Am. J. Cardiol. *90*, 22i-29i.

Pare, A., Dumont, M., Lemieux, I., Brochu, M., Almeras, N., Lemieux, S., Prud'homme, D., and Despres, J.P. (2001). Is the relationship between adipose tissue and waist girth altered by weight loss in obese men? Obes. Res. *9*, 526-534.

Porter, C., Herndon, D.N., Bhattarai, N., Ogunbileje, J.O., Szczesny, B., Szabo, C., Toliver-Kinsky, T., and Sidossis, L.S. (2015). Severe Burn Injury Induces Thermogenically Functional Mitochondria in Murine White Adipose Tissue. Shock *44*, 258-264.

Saeed, A.I., Sharov, V., White, J., Li, J., Liang, W., Bhagabati, N., Braisted, J., Klapa, M., Currier, T., Thiagarajan, M., et al. (2003). TM4: a free, open-source system for microarray data management and analysis. Biotechniques *34*, 374-378.

Shinoda, K., Luijten, I.H., Hasegawa, Y., Hong, H., Sonne, S.B., Kim, M., Xue, R., Chondronikola, M., Cypess, A.M., Tseng, Y.H., et al. (2015). Genetic and functional characterization of clonally derived adult human brown adipocytes. Nat. Med. *21*, 389-394.

Sidossis, Labros S., Porter, C., Saraf, Manish K., Børsheim, E., Radhakrishnan, Ravi S., Chao, T., Ali, A., Chondronikola, M., Mlcak, R., Finnerty, Celeste C., et al. (2015). Browning of Subcutaneous White Adipose Tissue in Humans after Severe Adrenergic Stress. Cell Metab *22*, 219-227.

Sidossis, L.S., Stuart, C.A., Shulman, G.I., Lopaschuk, G.D., and Wolfe, R.R. (1996). Glucose plus insulin regulate fat oxidation by controlling the rate of fatty acid entry into the mitochondria. J Clin Invest *98*, 2244-2250.

Wolfe, R.R., and Chinkes, D.L. (2005). Isotope tracers in metabolic research: principles and practice of kinetic analysis. (John Wiley & Sons).